Biosensors and Bioelectronics 25 (2010) 2627–2632

Contents lists available at ScienceDirect

Biosensors and Bioelectronics

journal homepage: www.elsevier.com/locate/bios

A novel mediator-free biosensor based on co-intercalation of DNA and hemoglobin in the interlayer galleries of α-zirconium phosphate

Limin Liu, Bo Shen, Jianjun Shi, Fang Liu*, Guo-Yuan Lu, Jun-Jie Zhu*

Key Laboratory of Analytical Chemistry for Life Science, Ministry of Education of China, School of Chemistry and Chemical Engineering, Nanjing University, Hankou Road 22, Nanjing 210093, PR China

ARTICLE INFO

Article history:
Received 1 February 2010
Received in revised form 21 April 2010
Accepted 21 April 2010
Available online 29 April 2010

Keywords:
Hemoglobin (Hb)
DNA
DNA/Hb/α-ZrP composite
Direct electron transfer (DET)

ABSTRACT

A novel mediator-free biosensor was constructed by the co-intercalation of negatively charged DNA and positively charged hemoglobin (Hb) in the interlayer galleries of layered α-zirconium phosphate (α-ZrP) with the delamination-assembly procedure at pH 5.5. X-ray diffraction and field-emission scanning electron microscopy results revealed the featured layered structure for the re-assembled DNA/Hb/α-ZrP composite. Infrared spectroscopy and circular dichroism results confirmed the coexistence of Hb and DNA in the composite and the considerably retained protein conformation of intercalated Hb. The direct electron transfer of Hb was facilitated by the co-intercalation of DNA and Hb. Because of the synergistic effect of α-ZrP host and co-intercalated DNA guest, the DNA/Hb/α-ZrP modified electrode exhibited good electrocatalytic response to H_2O_2 with higher sensitivity of 0.79 A M^{-1} cm^{-2} and lower detection of 4.28×10^{-7} M in the linear range of 7.28×10^{-7} to 9.71×10^{-5} M. Furthermore, the electrocatalytic activity of Hb in the DNA/Hb/α-ZrP composite retained at high temperature (85 °C) or in the presence of organic solvent (CH_3CN), which could be the protection of α-ZrP nanosheets.

1. Introduction

The biosensors based on the direct electron transfer of redox protein or enzyme have attracted considerable attention, because it can overcome the drawbacks of high applied potential and various interfering reactions (Gorton et al., 1999; Ghindilis et al., 1997). However, the direct electron transfer between redox protein or enzyme and the underlying electrodes is generally difficult, due to the deep embedding of electroactive center within a protective protein shell or the unfavorable orientation of adsorbed proteins on the electrode surface (Heller, 1990; Armstrong et al., 1988). Therefore, great efforts have been devoted in order to improve the communication between electroactive center and electrodes. Although grafting electron relays into protein structure (Willner and Katz, 2000; Xiao et al., 2003) can provide fast electron transfer rate, the complicated procedure usually limits its broad application. Accordingly, other strategy, especially the immobilization of redox protein in suitable matrixes, such as biomembrane-like films (Han et al., 2002; Rusling and Nassar, 1993), polymers (Cosnier et al., 1994; Lu et al., 2007), mesoporous silica (Wu et al., 2007; Dai et al., 2004), metal oxide nanoparticles (Feng et al., 2006; Topoglidis et al., 2001), inorganic clays (Mousty, 2004), etc. were widely adopted to enhance the heterogeneous electron transfer of proteins.

Compared with other supporting matrixes, inorganic layered solids show notable advantages. The regular layered structure and expandable interlayer space are suitable for accommodating biomolecules with different dimensions. Moreover, the strong mechanical strength, high thermal stability and intrinsically chemical inertia are favorable to the protection intercalated enzyme from disturbing by the environmental variations. In previous work, a variety of inorganic layered solids were used as supporting matrix for protein immobilization. For example, the enzyme electrodes based on the layered double hydroxides (LDHs) exhibited remarkable properties of high sensitivity, low K_M^{app} and good storage stability (Shan et al., 2003; Cosnier et al., 2006). The direct electron transfer of hemoglobin, myoglobin, horseradish peroxidase and cytochrome were achieved by intercalating proteins into layered titanate (Zhang et al., 2007a,b), niobate (Gao and Gao, 2007), bentonite (Zhou et al., 2002) or montmorillonite clay (Shumyantseva et al., 2004). Recently, α-ZrP, a negatively charged layer solid, has attracted extensive attention due to its excellent property for protein intercalation. These re-assembled protein/α-ZrP composites exhibited enhanced enzymatic activity or improved thermal stability, displaying the potential applications in biocatalysis (Kumar and Chaudhari, 2000, 2002).

* Corresponding authors. Tel.: +86 25 83685613; fax: +86 25 83685613.
E-mail addresses: liufang@nju.edu.cn (F. Liu), jjzhu@nju.edu.cn, jjzhu@netra.nju.edu.cn (J.-J. Zhu).

0956-5663/$ – see front matter © 2010 Elsevier B.V. All rights reserved.
doi:10.1016/j.bios.2010.04.031

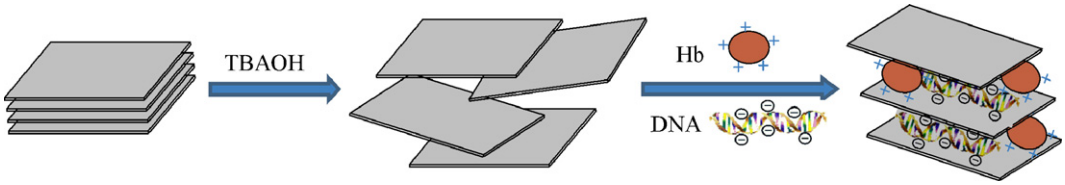

Scheme 1. Illustration of the co-intercalation of negatively charged DNA and positively charged Hb in layered α-ZrP.

Although a variety of attempts have been performed for the protein/ZrP based biosensors (Feng et al., 2005; Yang et al., 1998) and the direct electron transfer of redox proteins in ZrP matrix (Liu et al., 2008; Zhang et al., 2008; Yang et al., 2008), the relatively weak conductivity of ZrP limits the electrochemical performance of the biosensors. Recently, co-intercalation of DNA into α-ZrP improved the bioactivity of protein (Bhambhani and Kumar, 2006). However, the enhanced effect of co-intercalated DNA on the electrochemical performance of redox protein immobilized in layered solids has never been focused. Although DNA is not an electroactive species, charge migration within the DNA duplex have been confirmed, which is possible over distance up to 40 Å (Holmlin et al., 1997). This suggests DNA has a structurally inherent potential to facilitate the electron transfer of protein (Nassar and Rusling, 1996; Chen et al., 2000).

Herein, the synergistic effect of α-ZrP host and co-intercalated DNA guest was used to improve the electrochemical performance of Hb. A novel mediator-free biosensor was constructed by the co-intercalation of negatively charged DNA and positively charged hemoglobin in the interlayer galleries of layered α-ZrP with the delamination-assembly procedure at pH 5.5 as shown in Scheme 1. The direct electron transfer of Hb was facilitated by the co-intercalation of DNA and Hb. Because of the synergistic effect of α-ZrP host and co-intercalated DNA guest, the DNA/Hb/α-ZrP modified electrode exhibited good electrocatalytic response to H_2O_2 with higher sensitivity of 0.79 A M^{-1} cm^{-2} and lower detection of 4.28×10^{-7} M in the linear range of 7.28×10^{-7} to 9.71×10^{-5} M. Furthermore, the electrocatalytic activity of Hb in DNA/Hb/α-ZrP composite retained at high temperature (85 °C) or in the presence of organic solvent (CH_3CN), it may be due to the protection effect from α-ZrP nanosheets.

2. Experimental

2.1. Materials

Hemoglobin from bovine blood (molecular weight, MW, 64458) and Salmon sperm DNA (D1626, approximately 2000 bp) were purchased from Sigma Chemical Co. Tetrabutylammoniumhydroxide (TBAOH) aqueous solution (10 wt%) was purchased from Shanghai Chemical Reagent Company. All other reagents were of analytical grade and used water in the experiments was deionized.

2.2. Synthesis and delamination of α-ZrP

α-ZrP was prepared following a modified procedure (Kumar and Chaudhari, 2000). 4.79 g of phosphoric acid in 75 mL water was added to 75 mL of $ZrOCl_2$ solution containing 2.42 g $ZrOCl_2 \cdot 8H_2O$ under stirring dropwise. Then, the mixture was heated and kept at 90 °C for 48 h. The white solid obtained *via* centrifugation was washed with deionized water and acetone, respectively. The α-ZrP solid was then dried overnight at 60 °C.

The delamination of α-ZrP was performed by sonicating 5 mL aqueous suspension containing α-ZrP (0.1 g) and TBAOH (0.17 g) for 1 h. The final concentration of exfoliated α-ZrP was approximately 20 mg mL^{-1}.

2.3. Preparation of DNA/Hb/α-ZrP and Hb/α-ZrP composites

100 μL of 2.0 mg mL^{-1} salmon sperm DNA stock solution (0.1% HAC, pH 5.5), 100 μL of 20 mg mL^{-1} exfoliated α-ZrP suspension and 200 μL of 2.0 mg mL^{-1} Hb (0.1% HAC, pH 5.5) were added into 2.6 mL of 0.1% HAC buffer solution (pH 5.5) with shaking in sequence. After 24 h of equilibration at room temperature, the sample was separated by centrifugation and the precipitate was washed by 0.1% HAC buffer (pH 5.5) twice. Then the solid was lyophilized for XRD and FTIR studies. For preparing the DNA/Hb/α-ZrP modified electrode, the lyophilized solid was dispersed thoroughly in 200 μL 0.1% HAC (pH 5.5) again. Hb/α-ZrP composite was prepared in a similar procedure, only with the salmon sperm DNA stock solution replaced by 0.1% HAC (pH 5.5).

2.4. Construction of the biosensors

Glassy carbon electrodes with 3 mm in diameter were polished with 1, 0.3, and 0.05 μm alumina powder, respectively, followed by sonication in acetone and doubly distilled water successively. Then, the electrodes were allowed to dry under nitrogen stream. The prepared DNA/Hb/α-ZrP suspension was shaken for 5 min before used, following 8 μL of the mixture was dropped on the surface of a glass carbon electrode and allowed to dry at room temperature, subsequently, 8 μL of 0.5% Nafion was dropped on the GCE surface to fix the DNA/Hb/α-ZrP.

2.5. Apparatus

Powder X-ray diffraction patterns were collected on a Philips X'pert X-ray diffractometer. SEM images were obtained by a field-emission scanning electron microscopy (FESEM, HITACHI S4800). Infrared spectroscopy measurements were recorded on a Bruker Fourier transform spectrometer (Vector 22). Circular dichroism spectra were detected on a Jasco 810 spectropolarimeter. Electrochemical measurements were conducted on a CHI660B workstation (Shanghai Chenhua, China). All electrochemical experiments were performed with a conventional three-electrode system, using a saturated calomel electrode as the reference, a platinum wire as the counter electrode and the modified glassy carbon electrode (GCE) as the working electrode. Buffer solutions were purged with highly purified nitrogen for 30 min prior to electrochemical experiments, and a nitrogen environment was maintained in the cell by continuously bubbling N_2 during the entire experiments.

3. Results and discussion

3.1. Characterization of DNA/Hb/α-ZrP composite

XRD patterns of the re-assembled samples are shown in Fig. 1A. The interlayer distance of pristine α-ZrP is 0.76 nm, corresponding to a diffraction peak at 2θ 11.749°. After the exfoliated α-ZrP was incubated with Hb, a lower angle diffraction peak was observed at 2θ 1.885°, with the interlayer distance of 4.68 nm. The increase of interlayer distance is 3.92 nm, which is smaller than the dimension

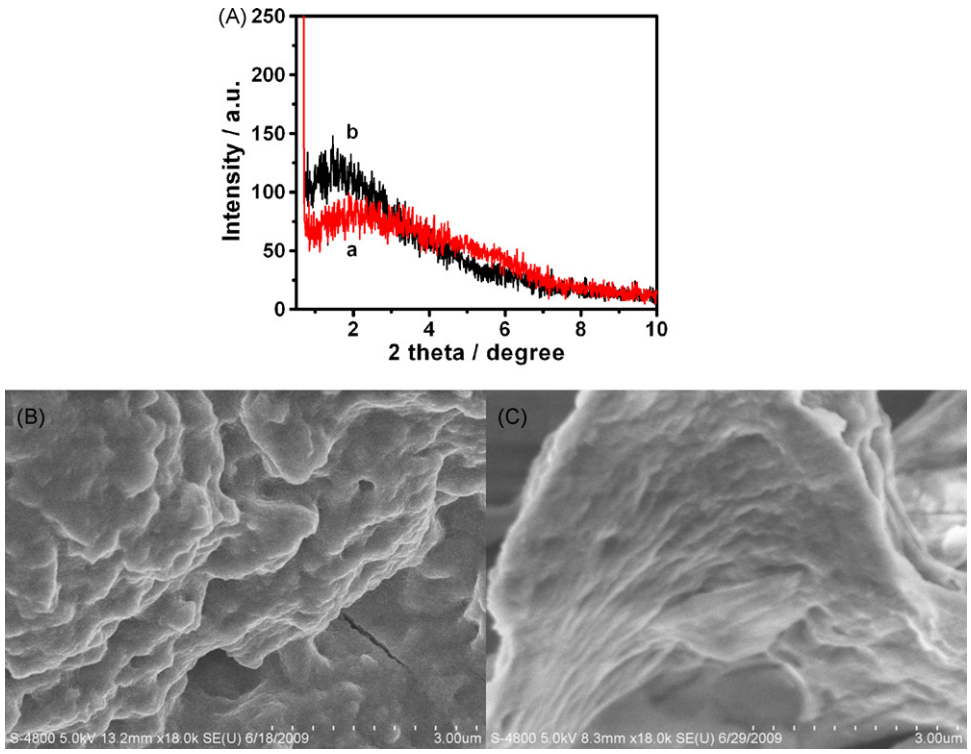

Fig. 1. (A) Powder XRD diffraction spectrogram of Hb/α-ZrP (a) and DNA/Hb/α-ZrP composite (b), (B) SEM image of α-ZrP and (C) SEM image of DNA/Hb/α-ZrP composite.

of Hb (5.3 nm × 5.4 nm × 6.5 nm), indicating that Hb is partial intercalated into the interlayer galleries of α-ZrP. The reason may be due to the large size of Hb and the small favorable interaction of protein with the support matrix (Patil et al., 2005; Zhou et al., 2002). When the exfoliated α-ZrP was incubated with Hb in the presence of DNA, the interlayer distance of re-assembled precipitates turned into 6.07 nm, corresponding to a low angle diffraction peak at 2θ 1.445°. The increase (5.31 nm) of interlayer distance was larger than both the expanded *d*-spacing (3.92 nm) when Hb was intercalated alone and the thickness (~2 nm) of a DNA monolayer (Choy et al., 2000; Patil et al., 2007), indicating that the interlayer spaces could be shared by DNA and Hb. Because of having the same negative charge of DNA and α-ZrP at pH 5.5, it could be presumed that the presence of positively charged Hb facilitated the intercalation of negatively charged DNA into the interlayer galleries of negatively charged α-ZrP, and formed the ternary composite of DNA/Hb/α-ZrP. The SEM image of α-ZrP in Fig. 1B shows the characteristic morphology of layered structure. In the case of DNA/Hb/α-ZrP composite, the layered feature is also observed as shown in Fig. 1C.

FTIR absorption spectra also confirmed the formation of DNA/Hb/α-ZrP ternary composite. In Fig. 2A, FTIR spectra of the lyophilized solid display all the characteristic absorbance of Hb, DNA, and α-ZrP. The absorbance bands at 1655 and 1543 cm^{-1} attribute mainly to the stretch of polypeptide amide I and amide II of Hb, respectively. Compared with Hb/α-ZrP, the enhanced intensity of amide I at 1655 cm^{-1} is partly attributed to the C=O stretch of bases in DNA, and the slight shift of amide II from 1539 to 1543 cm^{-1} suggests the electrostatic interaction between Hb and DNA. Moreover, the absorbance band at 1220 cm^{-1} can be assigned to the stretching vibration of P=O in DNA, while the strong and broad band from 1100 to 900 cm^{-1} can be attributed to the stretching vibration of P–O in both α-ZrP and DNA.

The results of UV characterization indicated further the interaction of DNA, Hb and α-ZrP. As shown in Fig. S1, the soret band of native Hb is located at 405 nm. After Hb combined with α-ZrP, the characteristic band of Hb shifts into 396 nm, and the intensity weakens significantly. In the case of DNA/Hb/α-ZrP ternary composite, the characteristic band of intercalated Hb is almost identical to that of Hb/α-ZrP. However, an additional band around 260 nm

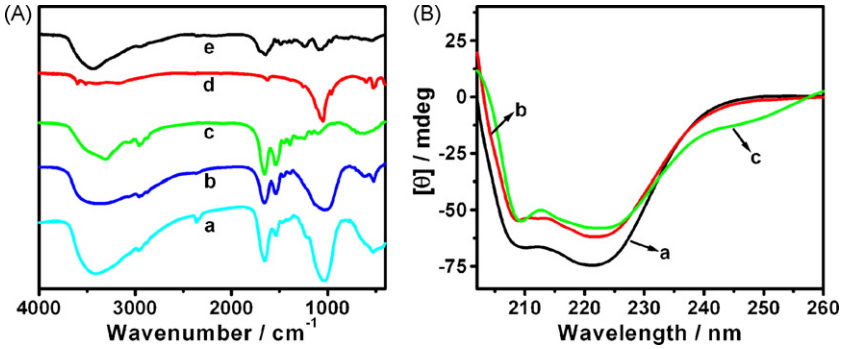

Fig. 2. (A) FTIR spectrogram of DNA/Hb/α-ZrP composite (a), Hb/α-ZrP (b), Hb (c), α-ZrP (d) and DNA (e) and (B) CD spectrogram of Hb (a), Hb/α-ZrP (b), DNA/Hb/α-ZrP composite (c).

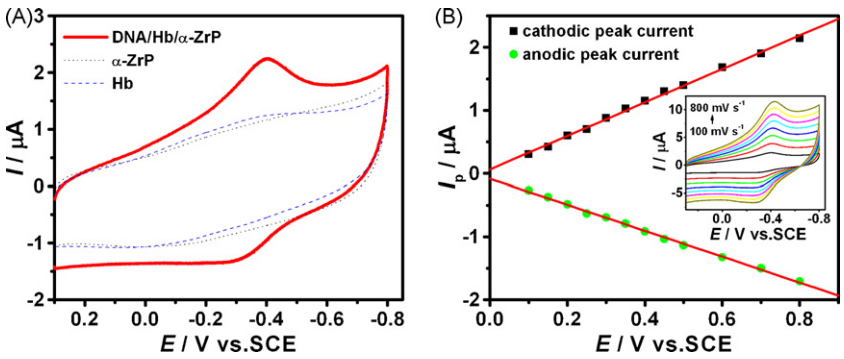

Fig. 3. (A) CVs of DNA/Hb/α-ZrP composite, Hb and α-ZrP modified electrode at 100 mV s^{-1} and (B) plots of cathodic and anodic peak current versus scan rate and CVs of DNA/Hb/α-ZrP electrode at scan rate of 100, 200, 300, 400, 500, 600, 700, 800 mV s^{-1} in 67 mM pH 7.0 PBS solutions (insert).

is observed, which is mainly attributed to the co-intercalated DNA.

The possible change in protein conformation after Hb bound with DNA in α-ZrP was monitored by CD absorption. In Fig. 2B, native Hb exhibits strong negative CD bands at 210 and 221 nm, which are the characteristic of α-helical structure of protein (Patil et al., 2005). Compared with native Hb, the Hb/α-ZrP composite presents a similar CD spectra profile, only slight decrease on intensity of the dual bands, indicating that the protein secondary structure was influenced to a small extent after Hb was intercalated into the interlayer galleries of α-ZrP. As for the DNA/Hb/α-ZrP composite, the dual CD bands at 209 and 222 nm are almost comparable to that of Hb/α-ZrP, while the slight deviation around 250 nm can be attributed to the weak CD of DNA. These results suggested that the protein secondary structure of intercalated Hb within DNA/Hb/α-ZrP composite was not further lost, compared with Hb/α-ZrP.

3.2. Electrochemical properties of the DNA/Hb/α-ZrP electrode

Fig. 3A shows the cyclic voltammograms (CVs) of different electrodes in 67 mM phosphate buffer solution (PBS, pH 7.0). No redox peaks were observed at the electrode modified by pre-exfoliated α-ZrP, indicating that α-ZrP was nonelectroactive. After the electrode was modified with Hb, an irreversible small reduction peak was observed, suggesting that the direct electron transfer was difficult between Hb and the electrode. However, after the electrode was modified with DNA/Hb/α-ZrP composite, a couple of quasi-reversible and well defined redox peaks at −334 and −405 mV were observed, with an apparent formal peak potential (E_p) of −370 mV and a peak-to-peak separation (ΔE_p) of 71 mV. The results provided the strong evidences for Hb direct electrochemistry by co-intercalating Hb and DNA into the interlayer galleries of α-ZrP.

The effect of scan rate on the response of the DNA/Hb/α-ZrP electrode is shown in Fig. 3B. With the increase of scan rate from 100 to 800 mV s^{-1}, both the reduction and oxidation peak currents (I_p) increase linearly, suggesting a surface-controlled process (Bard and Faulkner, 2001). For thin-layer electrochemistry, the surface concentration of electroactive Hb (Γ^*) at electrode can be estimated according to Faraday's law, $Q = nFA\Gamma^*$. Where F is Faraday constant, Q can be obtained by integrating the reduction peak of Hb, n and A stand for the electron transfer number and the area of electrode surface, respectively. The surface concentration of electroactive Hb (Γ^*) at the DNA/Hb/α-ZrP electrode was estimated to be 9.69×10^{-10} mol cm^{-2}, which was much lager than the theoretical monolayer coverage of Hb (1.89×10^{-11} mol cm^{-2}) (Wang et al., 2005). The highly surface concentration suggested the more effective immobilization of Hb in α-ZrP matrix due to the expandable interlayer space, and a multilayer of proteins participated in the electron transfer process.

The small peak-to-peak separation indicated a fast electron transfer rate. According to Laviron's theory (Laviron, 1979), when the peak-to-peak separation was less than 200 mV, the electron transfer rate constant k_s could be estimated according to the formula $k_s = mnFv/RT$, where m is a parameter related to the peak-to-peak separation, n the number of transferred electron, F the Faraday constant (C mol^{-1}), v the scan rate (V s^{-1}), T the temperature (K) and R is the universal gas constant (J mol^{-1} K^{-1}). The peak-to-peak separation is 71, 80, 87 and 96 mV at 100, 200, 300 and 400 mV s^{-1}, corresponding to the m of 0.4089, 0.3469, 0.3082 and 0.2675, respectively. The average k_s value can be calculated to be 3.0 ± 1.34 s^{-1}, which is larger than that of the Hb immobilized on other inorganic matrix, such as mesoporous silica (Dai et al., 2004), tungsten oxide (Feng et al., 2006) and niobate (Gao and Gao, 2007).

The direct electrochemistry of DNA/Hb/α-ZrP composite exhibited a strong dependence on the medium pH. An increase of medium pH caused a negative shift in the reduction and oxidation peaks potential. Moreover, all changes in voltammetric peak potentials with pH were reversible. In the range of medium pH from 5.0 to 8.0, the plot of apparent formal peak potential (E_p) versus pH is linear with a slop of −45 mV pH^{-1}. This value is slightly smaller than the theoretical value of −58 mV pH^{-1} at 25 °C for a reversible one-proton coupled single-electron transfer during electrochemical reduction (Nassar et al., 1997).

3.3. Electrocatalytic properties of the DNA/Hb/α-ZrP electrode

Hb has peroxidase activity and can be used to reduction H_2O_2 through electrochemical catalysis. The CVs of DNA/Hb/α-ZrP modified electrode in 67 mM PBS (pH 7.0) are shown in Fig. 4A. The cathodic peak (~−0.35 V) was increased after the addition of H_2O_2, and the corresponding anodic peak decreased. Furthermore, the reduction peak increased along with the increase of H_2O_2 concentration, indicating a typical electrocatalytic reduction process.

The reduction peak currents exhibited a linear response to H_2O_2 concentration. Herein, the increment of reduction peak current of DNA/Hb/α-ZrP electrode after addition of H_2O_2 was defined as I_{cat}, and the value of I_{cat} was calculated by subtracting the reduction peak current in the absence of H_2O_2 (Fig. 4A, curve a) from the corresponding value in the presence of H_2O_2 (Fig. 4A, curve b–h). Fig. 4B shows the relationship between electrocatalytic current (I_{cat}) and H_2O_2 concentration in the range of 7.28×10^{-7} to 9.71×10^{-5} M. The linear regression equation is $y = 0.056x + 0.091$ μA ($n = 15$), with a correlation coefficient of 0.999. From the slope of 0.056 μA μM^{-1}, the detection limit is estimated to be 4.28×10^{-7} M (signal-to-noise ratio (S/N): 3), and the sensitivity is 0.79 A M^{-1} cm^{-2}. When H_2O_2 concentration is higher than 291 μM, the response is almost unchanged, showing a characteristic of Michaelis–Menten kinetic mechanism. The apparent Michaelis–Menten constant (K_M^{app}) can

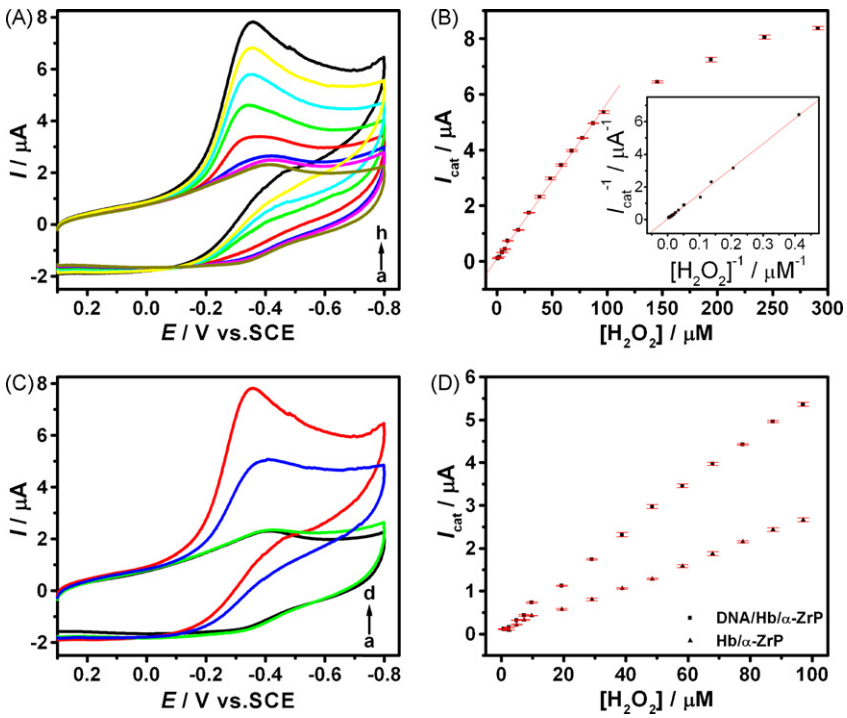

Fig. 4. (A) CVs of a DNA/Hb/α-ZrP electrode in 67 mM pH 7.0 PBS solutions with (a) 0 μM, (b) 0.73 μM, (c) 4.85 μM, (d) 19.41 μM, (e) 38.82 μM, (f) 58.23 μM, (g) 77.64 μM and (h) 97.05 μM H_2O_2 at 100 mV s^{-1}, (B) plot of electrocatalytic current (I_{cat}) versus H_2O_2 concentration for the DNA/Hb/α-ZrP electrode and the relative Lineweaver–Burk plot (Insert), (C) CVs of a DNA/Hb/α-ZrP electrode in 67 mM pH 7.0 PBS solutions with (a) 0 μM, (d) 97.05 μM and a Hb/α-ZrP electrode with (b) 0 μM, (c) 97.05 μM H_2O_2 and (D) plots of electrocatalytic current (I_{cat}) versus H_2O_2 concentration for the DNA/Hb/α-ZrP and Hb/α-ZrP electrode.

be calculated according to the Lineweaver–Burk equation (Kamin and Wilson, 1980).

$$\frac{1}{I_{ss}} = \frac{1}{I_{max}} + \frac{K_M^{app}}{I_{max}C}$$

where I_{ss} is the steady current after the addition of substrate, C the bulk concentration of the substrate and I_{max} is the maximum current measured under saturated substrate condition. In this work, I_{cat} is used as I_{ss} to obtain the Lineweaver–Burk plot. The K_M^{app} value of the modified electrode is calculated to be 458 μM, according to the Lineweaver–Burk plot (insert in Fig. 4B). This value is much smaller than that of Hb immobilized in layered niobate (Gao and Gao, 2007), Au-ZrP nanocomposite (Feng et al., 2005), kieselgubr film (Wang et al., 2002) and SP sephadex membrane (Fan et al., 2001), and also smaller than that of Mb immobilized in layered titanate (Zhang et al., 2007a,b), indicating a higher affinity to H_2O_2 and the good enzymatic activity to H_2O_2 reduction for the intercalated Hb within DNA/Hb/α-ZrP composite.

The effect of co-intercalated DNA on the electrocatalytic activity of Hb was investigated in concentration range of 7.27×10^{-7} to 9.71×10^{-5} M of H_2O_2. Fig. 4C indicates that the electrocatalytic reduction currents to H_2O_2 for the DNA/Hb/α-ZrP electrode are higher obviously than corresponding values of the Hb/α-ZrP electrode. Furthermore, the slope 0.056 μA $μM^{-1}$ of the linear relationship for the DNA/Hb/α-ZrP electrode is also higher than the value 0.026 μA $μM^{-1}$ of Hb/α-ZrP electrode (Fig. 4D). The results provided a strong evident that the co-intercalated DNA could enhance significantly the electrocatalytic activity of Hb.

The structure and bioactivity of enzyme is sensitive to temperature. However, previous researches indicated that bounding protein in inorganic layered materials or other solids could improve the thermal stability (Zhang et al., 2007a,b; Kumar and Chaudhari, 2003). In this work, the influence of temperature on the electrocatalytic activity of Hb was investigated, after thermal treatment for the modified electrode at different temperature for 15 min. The elevation of temperature almost keeps the electrocatalytic response to H_2O_2 as shown in Fig. 5A. At 85 °C, the electrocatalytic current decreases slightly by approximate 5%, compared with that of 35 °C (insert in Fig. 5A). In general, Hb denature at approximately 73 °C in solution (Kumar and Chaudhari, 2003). Therefore, the thermal stability of intercalated Hb within DNA/Hb/α-ZrP composite is significantly improved, and the reason may be due to the protection effect provided by outer α-ZrP nanosheets.

The application of biosensors in the detection of organic pollutants is often limited due to either the low stability and activity of enzyme in organic media or the insolubility of enzymatic substrates in aqueous environments. In general, inorganic materials have intrinsic advantages such as stronger mechanical strength and higher resistance to organic solvents. Therefore, the immobilization of enzyme into suitable inorganic supports appears to be an effective approach to overcome this problem (Wang et al., 2004a,b). Here, the influence of acetonitrile (CH_3CN) on electrocatalytic activity of DNA/Hb/α-ZrP electrode was investigated. As shown in Fig. 5B, when PBS (pH7.0) was replaced by a mix solution containing CH_3CN and PBS (pH7.0) with a volume ratio of 3:1, the electrocatalytic activity of Hb was considerably remained. Moreover, the electrocatalytic current increased linearly with the increase of H_2O_2 concentration, with a linear regression equation of $y = 0.039x + 0.55$ μA ($n = 11$, $R = 0.997$) in the range of 7.28×10^{-6} to 9.71×10^{-5} M (insert in Fig. 5B). The results suggested Hb entrapped within DNA/Hb/α-ZrP composite remained its bioactivity even in the presence of organic solvent, such as CH_3CN.

The reproducibility of the DNA/Hb/α-ZrP electrode was investigated, seven enzyme electrodes made at the same electrode independently showed an acceptable reproducibility with a relative standard deviation of 3.89% for the current detected at 29.1 μM H_2O_2. To investigate the stability of the DNA/Hb/α-ZrP electrode, the electrocatalytic response to 29.1 μM H_2O_2 was detected with

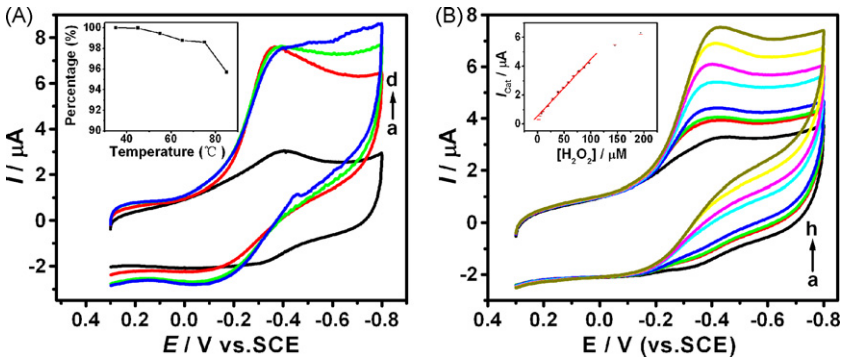

Fig. 5. (A) CVs of a DNA/Hb/α-ZrP electrode in 67 mM pH 7.0 PBS solutions without H_2O_2 (a) and with 97.05 μM H_2O_2 after the electrode thermally treated at (b) 35 °C, (c) 75 °C and (d) 85 °C for 15 min, and the plot of influence of temperature on the remained activity of Hb (insert); (B) CVs of a DNA/Hb/α-ZrP electrode in a mixture solution (CH_3CN: PBS = 3:1) with (a) 0 μM, (b) 7.23 μM, (c) 9.71 μM, (d) 19.41 μM, (e) 38.82 μM, (f) 58.23 μM, (g) 77.64 μM and (h) 97.05 μM H_2O_2, and the plot of electrocatalytic current (I_{cat}) versus H_2O_2 concentration (insert).

the storage time every 5 days. When the electrode was not in use, it was stored in air at room temperature. The retained current response up to 5 and 10 days were 98.1% and 94.7%, respectively, compared with the initial current response.

4. Conclusion

A novel mediator-free biosensor based on DNA/Hb/α-ZrP composite was fabricated by co-intercalating of negatively charged DNA and positively charged Hb into the interlayer galleries of negatively charged α-ZrP nanosheets. Attributing to the synergistic effect provided by α-ZrP host and co-intercalated DNA guest, the DNA/Hb/α-ZrP composite modified electrode demonstrated the direct electron transfer of Hb and the good electrocatalytic response to H_2O_2. These versatile properties, such as higher sensitivity of 0.79 A M^{-1} cm^{-2} and lower detection of 4.28×10^{-7} M, along with the retained electrocatalytic activity at high temperature (85 °C) or in the presence of organic solvent (CH_3CN), make this DNA/Hb/α-ZrP composite be a promising candidate for constructing the third generation electrochemical biosensor.

Acknowledgments

This work was supported financially by National Natural Science Foundation of China (Nos. 20635020, 20774039, 20872061). We also thank for the help from Jinggangshan University.

Appendix A. Supplementary data

Supplementary data associated with this article can be found, in the online version, at doi:10.1016/j.bios.2010.04.031.

References

Armstrong, F.A., Hill, H.A.O., Walton, N.J., 1988. Acc. Chem. Res. 21, 407–413.
Bard, A.J., Faulkner, L.R., 2001. Electrochemical Methods—Fundamentals and Applications, second ed. Wiley, New York.
Bhambhani, A., Kumar, C.V., 2006. Adv. Mater. 18, 939–942.
Chen, X., Ruan, C., Kong, J., Deng, J., 2000. Anal. Chim. Acta 412, 89–98.
Choy, J.-H., Kwak, S.-Y., Jeong, Y.-J., Park, J.-S., 2000. Angew. Chem., Int. Ed. 39, 4042–4045.
Cosnier, S., Innocent, C., Jouanneau, Y., 1994. Anal. Chem. 66, 3198–3201.
Cosnier, S., Mousty, C., Cui, X., Yang, X., Dong, S., 2006. Anal. Chem. 78, 4985–4989.
Dai, Z., Liu, S., Ju, H., Chen, H., 2004. Biosens. Bioelectron. 19, 861–867.
Fan, C., Wang, H., Sun, S., Zhu, D., Wagner, G., Li, G., 2001. Anal. Chem. 73, 2850–12850.
Feng, J.-J., Xu, J.-J., Chen, H.-Y., 2006. Electrochem. Commun. 8, 77–82.
Feng, J.-J., Xu, J.-J., Chen, H.-Y., 2005. J. Electroanal. Chem. 585, 44–50.
Gao, L., Gao, Q., 2007. Biosens. Bioelectron. 22, 1454–1460.
Ghindilis, A.L., Atanasov, P., Wilkins, E., 1997. Electroanalysis 9, 661–674.
Gorton, L., Lindgren, A., Larsson, T., Munteanu, F.D., Ruzgas, T., Gazaryan, I., 1999. Anal. Chim. Acta 400, 91–108.
Han, X., Huang, W., Jia, J., Dong, S., Wang, E., 2002. Biosens. Bioelectron. 17, 741–746.
Heller, A., 1990. Acc. Chem. Res. 23, 128–134.
Holmlin, R.E., Dandliker, P.J., Barton, J.K., 1997. Angew. Chem., Int. Ed. Engl. 36, 2714–2730.
Kamin, R.A., Wilson, G.S., 1980. Anal. Chem. 52, 1198–1205.
Kumar, C.V., Chaudhari, A., 2000. J. Am. Chem. Soc. 122, 830–837.
Kumar, C.V., Chaudhari, A., 2002. Chem. Commun., 2382–2383.
Kumar, C.V., Chaudhari, A., 2003. Micropor. Mesopor. Mater. 57, 181–190.
Laviron, E., 1979. J. Electroanal. Chem. 101, 19–28.
Liu, Y., Lu, C., Hou, W., Zhu, J.-J., 2008. Anal. Biochem. 375, 27–34.
Lu, Q., Zhou, T., Hu, S., 2007. Biosens. Bioelectron. 22, 899–904.
Mousty, C., 2004. Appl. Clay Sci. 27, 159–177.
Nassar, A-E.F., Rusling, J.F., 1996. J. Am. Chem. Soc. 118, 3043–3044.
Nassar, A-E.F., Zhang, Z., Hu, N., Rusling, J.F., Kumosinski, T.F., 1997. J. Phys. Chem. B 101, 2224–2231.
Patil, A.J., Muthusamy, E., Mann, S., 2005. J. Mater. Chem. 15, 3838–3843.
Patil, A.J., Li, M., Dujardin, E., Mann, S., 2007. Nano Lett. 7, 2660–2665.
Rusling, J.F., Nassar, A-E.F., 1993. J. Am. Chem. Soc. 115, 11891–11897.
Shan, D., Cosnier, S., Mousty, C., 2003. Anal. Chem. 75, 3872–3879.
Shumyantseva, V.V., Ivanov, Y.D., Bistolas, N., Scheller, F.W., Archakov, A.I., Wollenberger, U., 2004. Anal. Chem. 76, 6046–6052.
Topoglidis, E., Cass, A.E.G., O'Regan, B., Durrant, J.R., 2001. J. Electroanal. Chem. 517, 20–27.
Wang, S.-F., Chen, T., Zhang, Z.-L., Shen, X.-C., Lu, Z.-X., Pang, D.-W., Wong, K.-Y., 2005. Langmuir 21, 9260–9266.
Wang, H., Guan, R., Fan, C., Zhu, D., Li, G., 2002. Sens. Actuators B 84, 214–218.
Wang, Q., Gao, Q., Shi, J., 2004a. J. Am. Chem. Soc. 126, 14346–14347.
Wang, Q., Gao, Q., Shi, J., 2004b. Langmuir 20, 10231–10237.
Willner, I., Katz, E., 2000. Angew. Chem., Int. Ed. 39, 1180–1218.
Wu, S., Ju, H., Liu, Y., 2007. Adv. Funct. Mater. 17, 585–592.
Xiao, Y., Patolsky, F., Katz, E., Hainfeld, J.F., Willner, I., 2003. Science 299, 1877–1881.
Yang, F., Ruan, C., Xu, J., Lei, C., Deng, J., 1998. Fresen. J. Anal. Chem. 361, 115–118.
Yang, X., Chen, X., Yang, L., Yang, W., 2008. Bioelectrochemistry 74, 90–95.
Zhang, L., Zhang, Q., Li, J., 2007a. Adv. Funct. Mater. 17, 1958–1965.
Zhang, L., Zhang, Q., Lu, X., Li, J., 2007b. Biosens. Bioelectron. 23, 102–106.
Zhang, Y., Chen, X., Yang, W., 2008. Sens. Actuators B 130, 682–688.
Zhou, Y., Hu, N., Zeng, Y., Rusling, J.F., 2002. Langmuir 18, 211–219.